

Dissipative soliton resonance within different dispersion regimes in a single mode-locked laser

Zhetao Zhao(赵哲韬), Qinke Shu(舒沁珂), Ziyi Xie(解梓怡), Yuxuan Ren(任俞宣), Ying Zhang(张颖), Bo Yuan(袁博), Chunbo Zhao(赵春勃), Junsong Peng(彭俊松), and Heping Zeng(曾和平)

Citation: Chin. Phys. B, 2024, 33 (**7**): 074208. DOI: 10.1088/1674-1056/ad47b1
Journal homepage: http://cpb.iphy.ac.cn; http://iopscience.iop.org/cpb

What follows is a list of articles you may be interested in

A novel dual-channel thermo-optic locking method for the whispering gallery mode microresonator

Wenjie Fan(范文杰), Wenyao Liu(刘文耀), Ziwen Pan(潘梓文), Rong Wang(王蓉), Lai Liu(刘来), Enbo Xing(邢恩博), Yanru Zhou(周彦汝), Jun Tang(唐军), and Jun Liu(刘俊)
Chin. Phys. B, 2024, 33 (**5**): 054206. DOI: 10.1088/1674-1056/ad225f

On the generation of high-quality Nyquist pulses in mode-locked fiber lasers

Yuxuan Ren(任俞宣), Jinman Ge(葛锦蔓), Xiaojun Li(李小军), Junsong Peng(彭俊松), and Heping Zeng(曾和平)
Chin. Phys. B, 2024, 33 (**3**): 034210. DOI: 10.1088/1674-1056/acfa87

Spatiotemporal mode-locked multimode fiber laser with dissipative four-wave mixing effect

Ming-Wei Qiu(邱明伟), Chao-Qun Cai(蔡超群), and Zu-Xing Zhang(张祖兴)
Chin. Phys. B, 2022, 31 (**10**): 104207. DOI: 10.1088/1674-1056/ac6ee9

Generation of wide-bandwidth pulse with graphene saturable absorber based on tapered fiber

Ren-Li Zhang(张仁栗), Jun Wang(王俊), Mei-Song Liao(廖梅松), Xia Li(李夏), Pei-Wen Guan(关珮雯), Yin-Yao Liu(刘银垚), Yan Zhou(周延), Wei-Qing Gao(高伟清)
Chin. Phys. B, 2019, 28 (**3**): 034203. DOI: 10.1088/1674-1056/28/3/034203

Mode-locked fiber laser with $MoSe_2$ saturable absorber based on evanescent field

Ren-Li Zhang(张仁栗), Jun Wang(王俊), Xiao-Yan Zhang(张晓艳), Jin-Tian Lin(林锦添), Xia Li(李夏), Pei-Wen Kuan(关珮雯), Yan Zhou(周延), Mei-Song Liao(廖梅松), Wei-Qing Gao(高伟清)
Chin. Phys. B, 2019, 28 (**1**): 014207. DOI: 10.1088/1674-1056/28/1/014207

Dissipative soliton resonance within different dispersion regimes in a single mode-locked laser

Zhetao Zhao(赵哲韬)[1], Qinke Shu(舒沁珂)[1], Ziyi Xie(解梓怡)[1], Yuxuan Ren(任俞宣)[1], Ying Zhang(张颖)[1], Bo Yuan(袁博)[1], Chunbo Zhao(赵春勃)[2,†], Junsong Peng(彭俊松)[1,3,4,‡], and Heping Zeng(曾和平)[1,4,5]

[1] *State Key Laboratory of Precision Spectroscopy, East China Normal University, Shanghai* 200062, *China*
[2] *China Academy of Space Technology, Xi'an* 710100, *China*
[3] *Collaborative Innovation Center of Extreme Optics, Shanxi University, Taiyuan* 030006, *China*
[4] *Chongqing Key Laboratory of Precision Optics, Chongqing Institute of East China Normal University, Chongqing* 401120, *China*
[5] *Chongqing Institute for Brain and Intelligence, Guangyang Bay Laboratory, Chongqing* 400064, *China*

(Received 22 March 2024; revised manuscript received 22 April 2024; accepted manuscript online 6 May 2024)

Dissipative soliton resonance (DSR) was previously studied in separated mode-locked fiber lasers within different dispersion regimes including anomalous, near-zero and normal dispersion. Here we propose a method to study DSR in a single mode-locked laser in these different dispersion regimes. This is achieved by virtue of a waveshaper which can control the laser dispersion readily using software, avoiding the usual tedious cutback method. We find that dispersion has a negligible effect on DSR since the pulse duration keeps constant while dispersion is varied. Moreover, we examine the dynamics of DSR on the parameters of the SA including modulation depth and saturation power, and find that the pulse duration can be changed in a large range when the saturation power is decreased. Our numerical simulations could be important to guide relative experimental studies.

Keywords: mode locking, laser, fiber, pulse

PACS: 42.55.Wd, 42.65.–k, 42.65.Sf, 42.65.Re **DOI:** 10.1088/1674-1056/ad47b1

1. Introduction

Dissipative soliton resonance (DSR) refers to a stable flat-top square pulse, the pulse width of which increases linearly with pump strength.[1] DSR has attracted much attention because of its potential uses in materials processing,[2] sensing,[3,4] and microscopic imaging.[5] It was first observed experimentally in a passively mode-locked fiber laser with anomalous dispersion,[6] and its dynamics were later studied numerically using the Ginzburg–Landau equation which is an average model describing mode-locked lasers.[1,7,8]

Dispersion plays a significant role in the dynamics of dissipative solitons in mode-locked lasers.[9–17] It is therefore natural to ask whether dispersion is also important in the dynamics of DSR. So far, DSR has been investigated in different dispersion regions including anomalous, near-zero and normal dispersion.[18–25] However, it was generated in separated laser cavities, thus the role of dispersion on DSR is unknown. Generating DSR under different dispersion regimes in a single laser system is a challenging task as dispersion management is generally realized by changing the relative lengths of the different kinds of fibers inside the laser.[26–28]

Recently, a programmable spectral filter shows great advantages in dispersion management by software control, without varying the length of fibers.[29] It is also widely employed in mode-locked lasers, encompassing pulse shaping through dispersion management,[30] pulse synchronization,[31] enhancement of optical nonlinear effects,[32] pure-quartic soliton lasing[33] and Nyquist pulse generation.[34–38]

In this work, we propose a method to excite DSR in anomalous, normal and near-zero dispersion regimes in a single mode-locked laser, without changing the physical layout of the laser cavity. This is realized by employing a waveshaper such that the net dispersion of the laser can be readily varied using software. Our proposal is demonstrated using a discrete mode-locked laser model based on the nonlinear Schrödinger equation (NLSE).[39–42] We find that the DSR phenomenon is independent of dispersion. We also reveal how gain saturation energy, modulation depth and saturable power impact the dynamics of DSR.

2. Numerical model

The laser configuration is shown in Fig. 1. The power from a laser diode operating at 980 nm is injected into the ring laser through an optical wavelength division multiplexer (WDM). A 9-m erbium-doped fiber (EDF) with a group velocity dispersion of 40 ps^2/km serves as the gain medium. The net cavity dispersion can be changed from anomalous to normal dispersion regime, by changing the phase amplitude in a programmable waveshaper, which can also provide narrowband Gaussian-type spectral filtering. During this process, the

†Corresponding author. E-mail: zhaocb38@163.com
‡Corresponding author. E-mail: jspeng@lps.ecnu.edu.cn

© 2024 Chinese Physical Society and IOP Publishing Ltd

repetition frequency of the cavity remains unchanged because the length of the fiber is not changed. To achieve DSR mode locking, a saturable absorber (SA) such as nonlinear polarization rotation (NPR)[43] can be placed in the cavity. Other fibers in the ring cavity are 10 m highly nonlinear fiber (HNLF) and 27.07 m single-mode fiber (SMF), whose group velocity dispersion values are 0.64 ps^2/km and -23 ps^2/km, respectively. The employment of HNLF is to reduce the pump power threshold for DSR generation. 10% of the laser signal is outputted by a coupler.

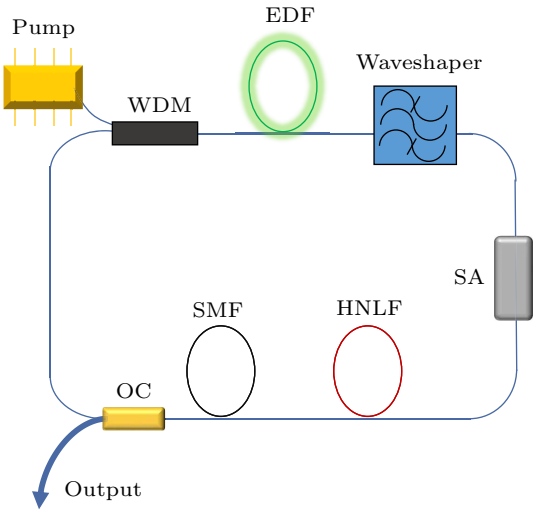


Fig. 1. Configuration of the mode-locked fiber laser. WDM: wavelength-division multiplexer; EDF: erbium-doped fiber; SA: saturable absorber; HNLF: highly nonlinear fiber; SMF: single-mode fiber; OC: optical coupler.

The transmission of the waveshaper is described by the following equation:[44]

$$H(\omega) = R(\omega)\exp\left[\frac{\mathrm{i}\beta_{2,\mathrm{acc}}\omega^2}{2}\right], \tag{1}$$

where $R(\omega)$ represents the profile of the filter and a Gaussian spectral profile $R(\omega) = \exp\left[-2(\omega/2\pi)^2/B^2\right]$ with a bandwidth (B) of 0.24 THz is used throughout the work. Second-order dispersion can be added through the term $\beta_{2,\mathrm{acc}}$ (in ps^2) in the spectral phase.

The pulse propagation in optical fibers can be numerical simulated with a generalized nonlinear Schrödinger equation (NLSE)[39,40]

$$\psi_z = -\frac{\mathrm{i}\beta_2}{2}\psi_{tt} + \mathrm{i}\gamma|\psi|^2\psi + \frac{g}{2}\left(\psi + \frac{1}{\Omega^2}\psi_{tt}\right), \tag{2}$$

where $\psi = \psi(z,t)$ is the slow-variation amplitude envelope with z being the moving coordinate, and β_2 and γ denote the group velocity dispersion and the Kerr nonlinear coefficient, respectively. The dissipation term includes gain having a parabolic profile with a bandwidth of Ω. The gain is saturated according to $g(z) = g_0/[1 + E(z)/E_{\mathrm{sat}}]$, where g_0 represents the small-signal gain, $E(z) = \int \mathrm{d}t\,|\psi|^2$ represents the energy of the pulse, and E_{sat} denotes the saturation energy of the gain which resembles the role of pump power in experiments.

The transmission curve for the SA is of the sine type[45] (Fig. 2), expressed as

$$T = T_0 + \Delta T \times \sin^2\left(\frac{\pi}{2} \times \frac{P}{P_{\mathrm{SA}}} + \varphi\right), \tag{3}$$

where T denotes the transmissivity, T_0 being the minimum transmittance, ΔT being the modulation depth, $P = \int |\psi|^2$ being the instantaneous pulse power, P_{SA} being the saturation power of the SA, and φ denotes the phase delay which for convenience is set to 0. The SA model described by Eq. (3) and Fig. 2 is not a general model for ordinary SAs, but a specialized model used to describe artificial SAs such as nonlinear optical loop mirror, nonlinear amplifying loop mirror and nonlinear polarization rotation.

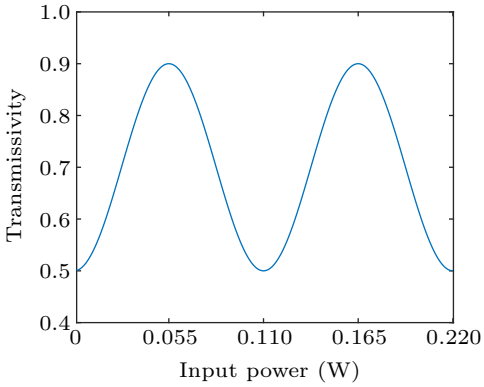


Fig. 2. A sine-type transmission curve of the saturable absorber.

3. Simulation results

The simulations in the following begin with a weak Gaussian single pulse, which has a temporal width of 1 ps, an energy of 0.1 fJ, and a central wavelength of 1575 nm. The small-signal gain g_0 of the gain fiber is set to 0.8 m^{-1}. The pulse evolution is modelled accurately by the split-step Fourier method.[46] Figure 3 shows the observed pulses in the DSR regime without altering the cavity's original net dispersion (-0.23 ps^2). The other parameters are shown in the caption of Fig. 3. DSR is evidenced by the rectangular pulse intensity profile and its broadening with gain saturation energy (Fig. 3(a)). As shown in Fig. 2, the peak power of the pulse is saturated by the sine-type transmission function of the saturable absorber. As a result, increasing the gain saturation energy (akin to the role of pump power in experiments) does not contribute to enhancing the power of the pulse, and the pulse broadens instead. The optical spectra of the pulses are shown in Fig. 3(b), showing that the spectral width narrows down as the gain saturation is increased.

Next, we change the net cavity dispersion by readily varying the term $\beta_{2,\mathrm{acc}}$ (in ps^2) in the spectral phase (Eq. (1)) while

the length of the fiber in the laser is fixed. The net cavity dispersion is changed to different regions including normal dispersion (1.4 ps^2), anomalous dispersion (-0.23 ps^2 and -1.4 ps^2) and near-zero dispersion (0.08 ps^2 and -0.08 ps^2). The parameters of SA are the same as that in obtaining Fig. 3 and the gain saturation energy is kept to be 2 pJ. The results are shown in Fig. 4. Figure 4(a) illustrates the pulse intensity profiles (solid line) and the corresponding chirp (dotted line) under different dispersion regions. Dispersion induced chirp can be clearly observed. The strong dispersion results in a large chirp (up- and down-chirp for -1.4 ps^2 and 1.4 ps^2, respectively). Such a large chirp means that the pulse leading and tailing edges contain different frequency components. Namely, the strong dispersion separates the low and high frequency components. As a result, the spectrum has two peaks under the strong dispersion regime (± 1.4 ps^2), as seen in Fig. 4(b).

The effect of the modulation depth of SA (ΔT) on DSR is also studied. In this case, ΔT is varied from 0.1 to 0.5, while the other parameters are kept constant. Figure 5 shows that the peak powers of the pulses are increased while the pulse widths are nearly invariant when the modulation depth is varied, resulting in an increase of the pulse energy. The reason for this process is that as the modulation depth increases, the transmittance of the SA is enhanced, giving rise to high-energy pulses. The corresponding optical spectra are shown in Fig. 5(b). As seen, with the increase of modulation depth of SA, the peak intensity of the optical spectra also increases.

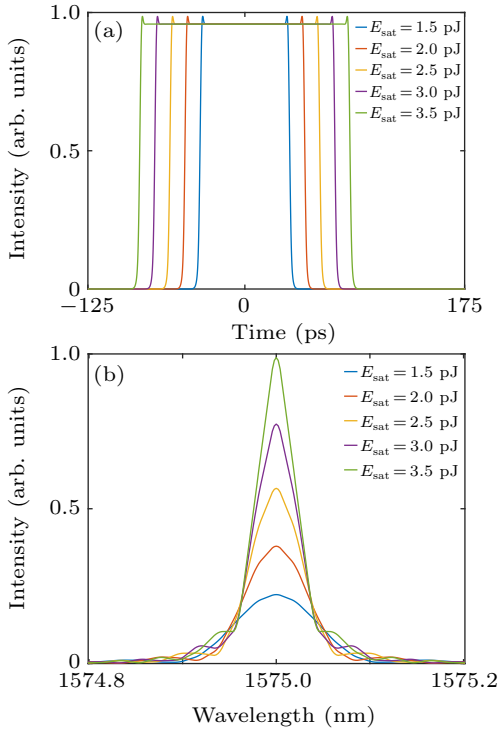


Fig. 3. (a) The pulse duration scaling with gain saturation energy. (b) The corresponding optical spectra. The parameters of net cavity dispersion, saturation power and modulation depth are -0.23 ps^2, 0.055 W, and 0.5, respectively.

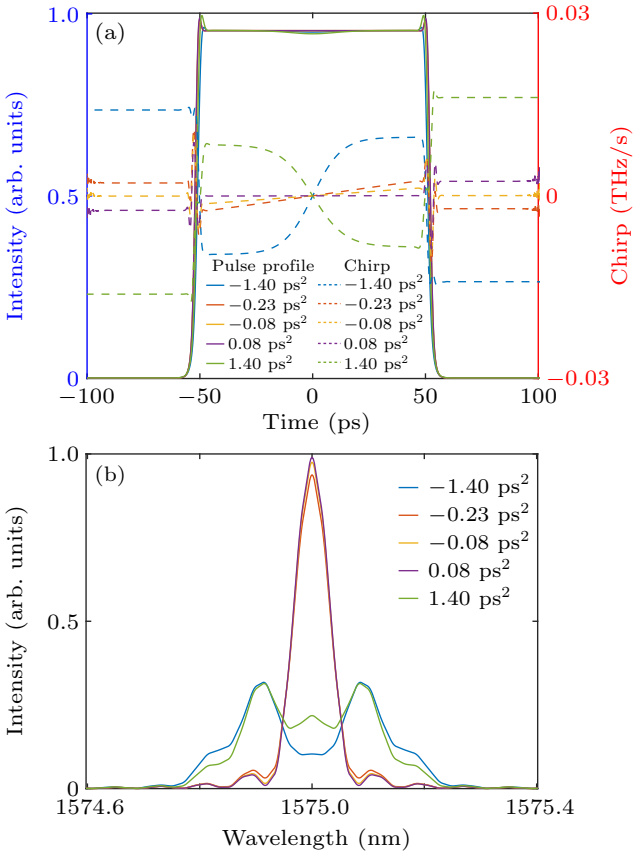


Fig. 4. (a) The pulse intensity profiles (solid line) and the corresponding chirp (dotted line) under different net cavity dispersion values. (b) The corresponding optical spectra. The parameters of saturation power, modulation depth, and gain saturation energy are 0.055 W, 0.5 and 2 pJ, respectively.

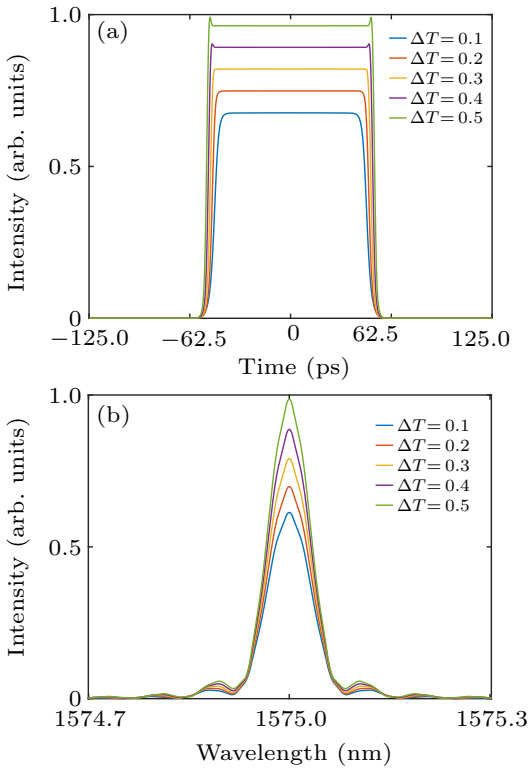


Fig. 5. (a) The temporal intensity of the pulses with different modulation depths. (b) The corresponding optical spectra. The other parameters used are $E_{sat} = 2$ pJ, $P_{SA} = 0.055$ W, and the net dispersion is -0.23 ps^2.

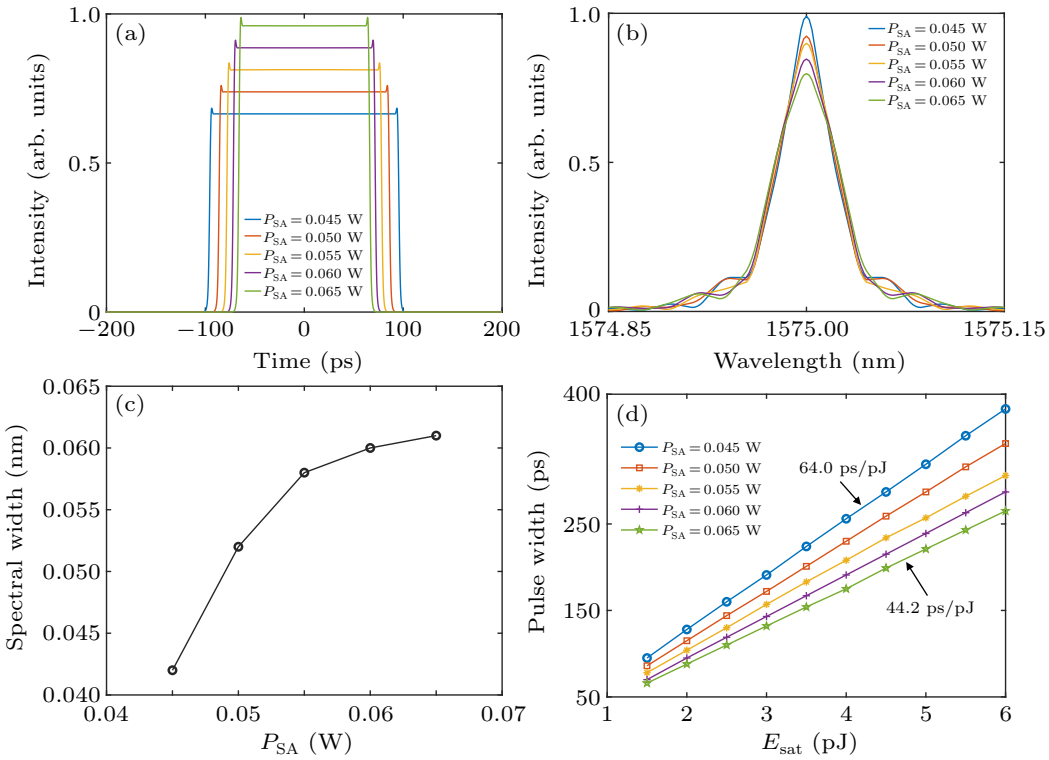


Fig. 6. (a) The pulse temporal profiles, (b) corresponding optical spectra and (c) optical spectral width at various saturation powers while other parameters are fixed. (d) The variation of pulse width by scaling the gain saturation energy for different saturation powers. The net cavity dispersion and modulation depth are -0.23 ps^2 and 0.5, respectively.

Besides modulation depth, the other parameter of SA-the saturation power (P_{SA}) is also varied to see the evolution of the pulses while the other system parameters are kept constant. Figure 6(a) depicts the evolution of the pulses as the saturation power is varied, which shows that the increase of saturation power leads to the increase of the pulse peak power and pulse narrowing. This result is due to the fact that the energy of the DSR pulse remains constant when the gain and losses of the laser are unchanged. The peak power of the DSR pulse increases as the saturation power increases, and the pulse narrows to keep a constant energy. The increase in peak power results in enhanced nonlinearity, thus the optical spectra are broadened when the saturation power is increased, as seen in Fig. 6(b). Figure 6(c) shows the spectral width increases with saturation power to highlight this broadening.

Since pulses with a tunable duration are crucial for many applications, it is necessary to investigate how to increase the sensitivity of pulse duration variation with respect to gain saturation energy. Figure 6(d) shows the pulse duration variation by scaling the gain saturation energy for different saturation powers of the SA. As seen, the pulse duration increases linearly with gain saturation energy. Moreover, the slope of the curves increases as the saturation power decreases. As an example, the slopes of the curve at the saturation power of 0.045 W and 0.065 W are 64.0 ps/pJ and 44.2 ps/pJ, respectively; namely, the former is 1.45 times the latter.

4. Conclusion

We achieve the exploration of DSR dynamics in different dispersion regimes within a single mode-locked fiber laser by incorporating a waveshaper capable of dispersion management using only software. We demonstrate that dispersion has a weak impact on DSR. However, very large dispersion causes the optical spectra of the pulse to be multiple peaked. We also reveal the effects of gain saturation energy, modulation depth, and saturation power on DSR dynamics. Our work could contribute to the understanding of DSR dynamics and thus may be beneficial to the design of light sources with rectangular profiles.

Acknowledgments

Project supported by the Innovation Program for Quantum Science and Technology (Grant No. 2023ZD0301000) and the National Natural Science Foundation of China (Grant Nos. 11621404, 11561121003, 11727812, 61775059, 12074122, 62022033, and 11704123). Sustainedly supported by the National Key Laboratory of Science and Technology on Space Microwave (Grant No. HTKT2022KL504008), the Shanghai Natural Science Foundation (Grant No. 23ZR1419000), and the National Key Laboratory Foundation of China (Grant No. 6142411196307).

References

[1] Chang W, Ankiewicz A, Soto-Crespo J and Akhmediev N 2008 *Phys. Rev. A* **78** 023830
[2] Hendow S T and Shakir S A 2010 *Opt. Express* **18** 10188
[3] Kalosha V, Ponomarev E, Chen L and Bao X 2006 *Opt. Express* **14** 2071
[4] Tan J, Zhong Z, Liu Y and Zeng D 2015 2015 *7th Asia-Pacific Conference on Environmental Electromagnetics (CEEM)* **2015** 7368632
[5] Evans R, Camacho-Lóez S, Pérez-Gutiérrez F and Aguilar G 2008 *Opt. Express* **16** 7481
[6] Matsas V J, Newson T P and Zervas M N 1992 *Opt. Commun.* **92** 61
[7] Chang W, Ankiewicz A, Soto-Crespo J M and Akhmediev N 2008 *J. Opt. Soc. Am. B* **25** 1972
[8] Chang W, Soto-Crespo J M, Ankiewicz A and Akhmediev N 2009 *Phys. Rev. A* **79** 033840
[9] Grelu P and Akhmediev N 2012 *Nat. Photonics* **6** 84
[10] Li X, Wang Y, Zhao W, Liu X, Wang Y, Tsang Y H, Zhang W, Hu X, Yang Z and Gao C 2012 *J. Lightwave Technol.* **30** 2502
[11] Huang X, Li X, Chen E, Pan Z, Guo P, Sun L, Wang Y and Zhao W 2024 *IEEE J. Sel. Top. Quantum Electron.* **2023** 3319342
[12] Liu X, Yao X and Cui Y 2018 *Phys. Rev. Lett.* **121** 023905
[13] Liu X and Pang M 2019 *Laser Photonics Rev.* **13** 1800333
[14] Liu X, Popa D and Akhmediev N 2019 *Phys. Rev. Lett.* **123** 093901
[15] Han Y, Guo Y, Gao B, Ma C, Zhang R and Zhang H 2020 *Prog. Quantum Electron.* **71** 100264
[16] Ma C, Wang C, Gao B, Adams J, Wu G and Zhang H 2019 *Appl. Phys. Rev.* **6** 041304
[17] Li Y Y, Gao B, Ma C Y, Wu G, Huo J Y, Han Y, Wageh S, Al-Hartomy O A, Al-Sehemi A G and Liu L 2023 *Laser Photonics Rev.* **17** 2200596
[18] Wu X, Tang D Y, Zhang H and Zhao L M 2009 *Opt. Express* **17** 5580
[19] Li J, Wang C and Wang P 2024 *Opt. Fiber Technol.* **82** 103637
[20] Lyu Y, Shi H, Wei C, Li H, Li J and Liu Y 2017 *Photonics Res.* **5** 612
[21] Li X, Liu X, Hu X, Wang L, Lu H, Wang Y and Zhao W 2010 *Opt. Lett.* **35** 3249
[22] Mei L, Chen G, Xu L, Zhang X, Gu C, Sun B and Wang A 2014 *Opt. Lett.* **39** 3235
[23] Chowdhury S D, Pal A, Chatterjee S, Sen R and Pal M 2018 *J. Lightwave Technol.* **36** 5773
[24] Armas-Rivera I, Cuadrado-Laborde C, Carrascosa A, Kuzin E, Beltrán-Pérez G, Díez A and Andrés M V 2016 *Opt. Express* **24** 9966
[25] Tang Y, Li F and Yu X 2022 *Optics Laser Technol.* **152** 108147
[26] Chernysheva M, Krylov A, Ogleznev A, Arutyunyan N, Pozharov A, Obraztsova E and Dianov E 2012 *Opt. Express* **20** 23994
[27] Ortaç B, Plötner M, Schreiber T, Limpert J and Tünnermann A 2007 *Opt. Express* **15** 15595
[28] Nishizawa N, Jin L, Kataura H and Sakakibara Y 2015 *Photonics* **2** 808
[29] Pulikkaseril C, Stewart L A, Roelens M A F, Baxter G W, Poole S and Frisken S 2011 *Opt. Express* **19** 8458
[30] Peng J and Boscolo S 2016 *Sci. Rep.* **6** 25995
[31] Mao D, Wang H, Zhang H, Zeng C, Du Y, He Z, Sun Z and Zhao J 2021 *Nat. Commun.* **12** 6712
[32] Lourdesamy J P, Runge A F, Alexander T J, Hudson D D, Blanco-Redondo A and de Sterke C M 2022 *Nat. Phys.* **18** 59
[33] Runge A F, Hudson D D, Tam K K, de Sterke C M and Blanco-Redondo A 2020 *Nat. Photonics* **14** 492
[34] Nakazawa M, Yoshida M and Hirooka T 2014 *Optica* **1** 15
[35] Xu K, Sung J Y, Wong C Y, Cheng Z, Chow C W and Tsang H K 2014 *Opt. Commun.* **329** 23
[36] Boscolo S, Finot C and Turitsyn S K 2015 *IEEE Photonics J.* **7** 7802008
[37] Yue L, Liu Y, Cai W, Cao D, Li Y and Wu J 2023 *Opt. Commun.* **533** 129308
[38] Ren Y, Ge J, Li X, Peng J and Zeng H 2024 *Chin. Phys. B* **33** 034210
[39] Haus H A 2000 *IEEE J. Sel. Top. Quantum Electron.* **6** 1173
[40] Agrawal G P 1990 *IEEE Photonics Technol. Lett.* **2** 875
[41] Peng J and Zeng H 2018 *Laser Photonics Rev.* **12** 1800009
[42] Peng J and Zeng H 2019 *Phys. Rev. Appl.* **11** 044068
[43] Peng J, Sorokina M, Sugavanam S, Tarasov N, Churkin D V, Turitsyn S K and Zeng H 2018 *Commun. Phys.* **1** 20
[44] Boscolo S, Finot C, Karakuzu H and Petropoulos P 2014 *Opt. Lett.* **39** 438
[45] Cheng Z, Li H and Wang P 2015 *Opt. Express* **23** 5972
[46] Agrawal G P 2019 *Nonlinear Fiber Optics* **50** 309